Journal of Insights in Basic and Applied Sciences

مجلة رؤى في العلوم الأساسية والتطبيقية

ISSN: 3106-1737

Volume 2, Issue 3, 2026, Pages: 403-421

Journal homepage: https://jibas.com.ly/index.php/jibas/en

Optimal Solar PV Module Specification Across Libya's Climate Zones: A Multi-Stress Analysis with PVsyst Cross-Validation, Integrating Thermal, Soiling, Humidity, and Wind Effects

Islam Shahboun [1]*, Abdulgader Alsharif [2]

[1] Mechanical and Industrial Eng. Department, faculty of Engineering, University of Tripoli, Tripoli, Libya

[2] Department of Electric and Electronic Engineering, College of Technical science Sabha, Sabha, Libya

المواصفة المثلى لألواح الطاقة الشمسية عبر المناطق المناخية في ليبيا: تحليل متعدد الإجهادات مع التحقق المتقاطع بواسطة *PVsyst* ، يدمج تأثيرات الحرارة والتلوث الغباري والرطوبة والرياح

إسلام شهبون[1]*، عبد القادر الشريف[2]

[1] قسم الهندسة الميكانيكية والصناعية، كلية الهندسة، جامعة طرابلس، طرابلس، ليبيا

[2] قسم الهندسة الكهربائية والالكترونية، كلية العلوم التقنية سبها، سبها، ليبيا

*Corresponding author: i.shahboun@uot.edu.ly

Received: June 22, 2026	Accepted: July 27, 2026	Published: August 12, 2026

Abstract:

Libya spans a coastal Mediterranean strip, a highland plateau, and a hyper-arid desert interior within one country, yet PV specifications are typically chosen without accounting for this diversity. This study derives three data-driven climate zones for Libya from twelve years of weather data at twelve stations, using k-means clustering of temperature, humidity, elevation, and irradiance. For each zone, thermal derating, soiling, humidity-based PID/corrosion risk, and wind effects were modeled using the Faiman cell-temperature formulation, Perez transposition, literature-derived soiling rates, and separated mean-wind cooling and extreme-gust design values. Thermal derating loss ranges from 3.39% in the coastal zone to 5.35% in the desert interior, while soiling loss at a 30-day cleaning cycle ranges from 2.70% to 8.25%. Combined heat-humidity stress hours reach 1119.8 h/yr in the coastal zone against 2.8 h/yr in the desert interior, and net specific yield differs by only 2.25% across zones under uniform 30-day cleaning but by 7.16% under a zone-appropriate schedule; to the authors' knowledge, this stress-hour contrast and cleaning-schedule impact are the first quantified evidence that Libya's climate zones differ more in maintenance and reliability requirements than in raw energy potential. Results were cross-validated against PVsyst 7.4.8 at three sites using an as-installed AIKO ABC module; PVsyst independently confirms the desert interior outproduces the coastal and highland zones despite higher losses. Findings combine into a specification matrix covering cell technology, PID mitigation, corrosion class, cleaning cycle, and wind rating, giving a practical basis for PV deployment across Libya.

Keywords: Photovoltaic Performance, Climate Zoning, Thermal Derating, Soiling, PID Risk, Wind Cooling, Pvsyst, Libya.

الملخص
تمتد ليبيا عبر شريط ساحلي متوسطي، وهضبة مرتفعة، وصحراء داخلية شديدة الجفاف ضمن بلد واحد، إلا أن مواصفات الألواح الشمسية (PV) تُختار عادة دون مراعاة هذا التنوع المناخي. تشتق هذه الدراسة ثلاث مناطق مناخية مبنية على البيانات لليبيا، اعتمادًا على اثني عشر عامًا من البيانات المناخية في اثنتي عشرة محطة رصد، باستخدام تحليل التجميع الإحصائي (k-means) لدرجة الحرارة والرطوبة والارتفاع والإشعاع الشمسي. ولكل منطقة، تم نمذجة الفاقد الحراري، والتلوث الغباري، ومخاطر التدهور الكهربائي المستحث بالجهد (PID) والتآكل المرتبطة بالرطوبة، وتأثيرات الرياح، باستخدام نموذج Faiman لحرارة الخلية الشمسية، وتحويل Perez للإشعاع، ومعدلات ترسّب غباري مستمدة من الأدبيات العلمية، مع فصل تأثير الرياح إلى مساهمة تبريدية بمتوسط سرعة الرياح وقيمة تصميمية إنشائية عند سرعات الرياح القصوى.
يتراوح الفاقد الحراري السنوي بين 3.39% في المنطقة الساحلية و5.35% في الصحراء الداخلية، بينما يتراوح فاقد الغبار عند دورة تنظيف كل 30 يومًا بين 2.70% و8.25%. وتصل ساعات الإجهاد الحراري-الرطوبي المشترك إلى 1119.8 ساعة/سنة في المنطقة الساحلية مقابل 2.8 ساعة/سنة فقط في الصحراء الداخلية، بينما لا يتجاوز الفارق في الإنتاجية النوعية الصافية بين المناطق 2.25% عند اعتماد جدول تنظيف موحّد كل 30 يومًا، ليتسع هذا الفارق إلى 7.16% عند اعتماد جدول تنظيف مخصص لكل منطقة؛ وهذا التباين في ساعات الإجهاد وتأثير جدول الصيانة يمثلان، على حد علم الباحثين، أول دليل كمّي على أن المناطق المناخية الليبية تختلف في متطلبات الصيانة والموثوقية أكثر من اختلافها في الإمكانات الشمسية الخام.
جرى التحقق من النتائج بشكل متقاطع مقابل برنامج PVsyst 7.4.8 في ثلاثة مواقع ممثّلة باستخدام لوح AIKO ABC المُركَّب فعليًا؛ ويؤكد PVsyst بشكل مستقل أن الصحراء الداخلية تتفوق إنتاجيًا على المنطقتين الساحلية والهضبية رغم ارتفاع فواقدها. وتُدمج هذه النتائج في مصفوفة مواصفات تغطي تقنية الخلية، وإجراءات مقاومة PID، وفئة مقاومة التآكل، ودورة التنظيف، وتصنيف مقاومة الرياح، لتوفر أساسًا عمليًا لقرارات نشر أنظمة الطاقة الشمسية عبر ليبيا.

الكلمات المفتاحية: أداء الألواح الشمسية، التصنيف المناخي، الفاقد الحراري، التلوث الغباري، مخاطر التدهور المستحث بالجهد (PID) ، تبريد الرياح، PVsyst، ليبيا

Introduction

The introduction should be typed in Times New Roman with font size 10. Author can select Normal style setting facilities, and community-level infrastructure across North Africa, and the choice of module technology, cleaning regime, and structural mounting is, in practice, an energy-system design decision for the built environment rather than a PV-technology decision made in isolation. In Libya, where grid-supplied electricity is unreliable, PV is frequently adopted at the scale of individual buildings and distributed facilities, so the specification decisions addressed in this study feed directly into how energy systems are planned and operated within the built environment across a climatically diverse country, and not only into standalone PV module performance.

Libya's electricity system depends heavily on fossil-fuel generation and has faced repeated supply shortages over the past decade, which has renewed interest in solar photovoltaic (PV) power as an alternative source [1]. The country holds substantial solar and wind resources, with annual global horizontal irradiation exceeding 2000 kWh/m² across large parts of the south [2]. Early feasibility work on PV reliability in southern Libyan cities dates back to Nassar and Salem [3], who reported favorable output despite the harsh desert environment.

Libya spans a wide range of climates within a single country: a humid Mediterranean coastline, a highland belt above 600 m, and a hyper-arid desert interior extending into the Sahara. Nassar et al. [4], [5] used Solargis weather data and the System Advisor Model to map suitable PV module and inverter types across Libyan territory, and found that treating the whole country under one specification produces avoidable losses, with savings of up to 45% possible when the module type is matched to the local climate. This finding motivates a Libya-specific inquiry into how climate zone should shape PV specification, rather than extrapolating results from one location to the entire country [4].

Subsequent Libyan case studies have examined individual sites or single stress factors rather than a national zoning scheme. Tawil and Gebrel [6] studied thermal performance mitigation for PV modules across three Libyan cities in different regions. Moodu [7] evaluated a 2 MW single-axis tracker plant in the hyper-arid climate of Traghn in the south. A geoclimatic analysis of 500 W panels was carried out for Qasr Bin Ghashir near Tripoli [8]. Alsharif [9] reviewed dust mitigation strategies specific to Libyan climate zones, and Elbaz and Elfaqih [10] measured dust accumulation losses in a Libyan coastal environment. Each of these studies isolates one location or one factor. None integrates thermal, soiling, humidity, and wind effects into a single zone-based specification framework.

Outside Libya, several frameworks have been proposed to classify climate for PV purposes. Ascencio-Vásquez et al. [11] adapted the Koppen-Geiger classification into a PV-specific scheme and mapped expected system performance worldwide. Huld and Amillo [12] showed that irradiance, air temperature, and wind speed together explain most of the regional variation in PV yield across large geographical areas. Bamisile et al. [13] reviewed the environmental factors that affect PV output at a global scale, and Adothu et al. [14] reviewed the performance, reliability, and testing-standard gaps specific to crystalline-silicon modules in desert climates. These frameworks operate at a coarse, multi-country resolution. None of them derives a station-based climate zoning specific to a single country from local weather data, which is the approach adopted in this study for Libya.

The choice of a thermal model for cell temperature prediction is supported by a substantial body of work. Kempe et al. [15] argued for new testing standards for modules operating in high-temperature micro-environments. Herrmann et al. [16] and Monokroussos et al. [17] examined the uncertainty and annual-yield impact of the IEC 61853 climate-specific energy rating standard. Oliveira et al. [18] validated thermal models for bifacial systems under varying albedo. Nyarko et al. [19] generated temperature-cycle profiles from in-situ climatic data to predict thermo-mechanical degradation, and Bevilacqua et al. [20] validated an accurate thermal model for PV generation across different climatic conditions over the long term. Elyaqouti et al. [21] presented a combined thermal and electrical model of PV modules, and Jaeckel et al. [22] compared mission profiles for Middle Eastern desert climates against temperate European conditions. Lamaamar et al. [23] evaluated several cell-temperature models under semi-arid conditions, and Aoun [24] tested free-standing module temperature outdoors under desert climate. This literature supports the use of an irradiance- and wind-dependent cell-temperature model, such as the Faiman formulation used in this study, over models that rely on ambient temperature alone.

Dust-related soiling losses have been measured across nearly every arid and semi-arid region bordering Libya. In Algeria, Memiche et al. [25] reported combined dust, soiling, aging, and weather effects in a Saharan environment, Dabou et al. [26] monitored a grid-connected system under different climatic conditions in the south, and Chabachi et al. [27] compared experimental and simulated performance in the southwest. In Morocco, Azouzoute et al. [28] modeled dust effects on fixed and tracking systems under semi-arid conditions, Ait Ali et al. [29] examined desert-region output together with the groundwater implications of panel-cleaning maintenance, Belmahdi and Bouardi [30] assessed solar potential with PVsyst in the northern zone, Ait Omar et al. [31] compared real yields against PVSYST simulations at four installations, and Abraim et al. [32] compared soiling effects on CSP and PV technologies under a semi-arid climate.

The Gulf states supply the largest body of soiling literature relevant to hyper-arid conditions. In Qatar, Guo et al. [33] and Javed et al. [34] documented dust and seasonal soiling variability in Doha over multiple years, Aïssa et al. [35] characterized the structural and physical properties of local dust particles, Touati et al. [36], [37] measured the combined effect of dust, relative humidity, and temperature on PV efficiency, and Jain et al. [38] modeled rooftop soiling and albedo losses using PVsyst and SAM. Hachicha et al. [39] reported dust impacts under United Arab Emirates weather conditions, Al Garni [40] quantified soiling losses in Saudi Arabia, and Adouane et al. [41] compared PV module technologies under Kuwait's harsh climate. In Oman, Al Siyabi et al. [42] measured soiling losses under desert conditions, and Chala et al. [43] studied the effect of Al Seeb's climate on panel performance.

Further afield, similar dust and soiling effects have been reported in Iraq, sub-Saharan Africa, and Central and South Asia. Chaichan et al. [44] reviewed sand and dust storm impacts on PV efficiency in Baghdad, Hameed et al. [45] analyzed the reliability of PV modules installed under Iraq's harsh climate, and Othman and Hatem [46] assessed outdoor PV performance against commercial software estimates in hot, dry conditions. Chanchangi et al. [47] linked soiling losses to weather parameters in northern Nigeria, Ndeto et al. [48] correlated dust deposits with wind speed and relative humidity in Kenya, and Salimi et al. [49] found a similar three-way interaction between dust concentration, wind speed, and relative humidity in Tehran. Xu et al. [50] showed that dust deposition changes the surface temperature of soiled glass under windy conditions, Toshov et al. [51] evaluated dust and ambient temperature effects in Uzbekistan, Andrea et al. [52] measured industrial dust deposition in a tropical region, and Elamim et al. [53], [54] studied dust accumulation under a Mediterranean climate.

Wind and humidity appear repeatedly in this literature as modifiers of soiling and thermal loss rather than as independently modeled factors. Mehdi et al. [54] showed experimentally that wind acts as a natural cooling agent for PV power plants in desert locations, consistent with the wind-dependent term used in the Faiman model. Stankov et al. [55] found that wind and rainfall together influence PV performance in a dusty environment, and Sher et al. [56] examined how various dust types combine with humidity to affect renewable energy module output. None of the studies reviewed builds a standalone humidity- or PID-risk indicator of the kind proposed in Section 3.4 of this study.

Finally, PVsyst has been used as an independent cross-validation tool in several of the studies above rather than as the sole modeling approach, a practice this study follows. Betti et al. [57] compared different PV simulation software packages directly against one another, Mashaly et al. [58] validated a stand-alone PV system design in PVsyst against experimental measurements, and Shirzad et al. [59] documented the design and development of a grid-connected PV plant in PVsyst. Building on this practice, the present study uses PVsyst as an independent check on the pvlib-based thermal model rather than as a replacement for it, and reports both results rather than treating either as ground truth.

Despite this large body of literature, no published study integrates thermal derating, dust soiling, humidity-driven degradation risk, and wind effects into a single climate-zone-based framework for module and system specification in Libya. The Libya-specific studies available [1-3,6-10] each cover one location or one stress factor. The climate-classification frameworks available [11,13,14] operate at a resolution too coarse to distinguish Libya's coastal, highland, and desert-interior zones from one another. The soiling literature is extensive across the wider MENA region and the Gulf [25-53] but has not previously been combined with a locally derived thermal model to build a zone-specific module specification matrix for Libya.

In this study, 12 years of typical-meteorological-year weather data from 12 Libyan stations were used to derive three data-driven climate zones through statistical clustering of temperature, relative humidity, elevation, and irradiance. For each zone, thermal derating was modeled using the Faiman cell-temperature formulation with Perez plane-of-array transposition, soiling losses were estimated from literature-derived deposition rates under a range of cleaning intervals, a humidity-based proxy for PID and corrosion risk was constructed from combined heat-humidity stress hours, and wind effects were separated into a mean-wind cooling contribution and an extreme-gust structural design value. The resulting zone-specific results were cross-validated against PVsyst 7.4.8 simulations at three representative sites using an as-installed AIKO ABC module and matched thermal-loss parameters. The paper is organized as follows: Section 2 describes the data and methodology; Section 3 presents the results for each stress factor and the resulting zone-specific specification matrix; Section 4 reports the PVsyst cross-validation; and Section 5 discusses the study's limitations and the research still required before field deployment.

Methodology

Study Area and Weather Data

Twelve locations were selected across Libya to capture the country's full range of latitude, elevation, and distance from the Mediterranean coast: Tripoli, Zuwara, Derna, Misrata, and Benghazi on the coast; Gharyan, Yefran, and Hamada on the western highland plateau; and Ghadamis, Sabha, Awbari, and Kufra in the desert interior. Typical meteorological year (TMYx) data covering 2011-2025 were obtained for each station, giving 8760 hourly records of dry bulb temperature, relative humidity, wind speed, and global, direct normal, and diffuse horizontal irradiance per station per year.

Climate Zone Classification

A data-driven climate zoning was derived instead of applying a generic Koppen-Geiger classification [11], because a station-based approach reflects the local station network directly rather than a global climate boundary drawn at a coarser resolution. For each station, four annual metrics were computed from the TMYx data: mean dry-bulb temperature, mean relative humidity, elevation, and annual global horizontal irradiation. The four metrics were standardized and passed to a k-means clustering algorithm with three clusters. The algorithm assigned five stations to a coastal Mediterranean zone (Zone A), three stations to a highland transitional zone (Zone B), and four stations to a desert interior zone (Zone C). Hamada, at 623 m elevation, clustered with Zone B on the elevation axis despite a relative humidity (36.6%) closer to the Zone C range, and is treated in the results as a transitional case within Zone B rather than reassigned.

Plane-of-Array Irradiance and Cell Temperature

Solar position was computed for each hour and station using the pvlib Python library [60]. Plane-of-array (POA) irradiance was obtained from the direct, diffuse, and global horizontal components using the Perez transposition model [61], with the array tilted at the station latitude (capped at 40°), oriented due south, and a ground albedo of 0.20. Cell temperature was then computed from the POA irradiance, ambient temperature, and wind speed using the Faiman thermal model [62]:

$$T_{cell} = T_{amb} + \frac{POA}{U_c + U_V \times WS}$$

Two parameter sets were used at different stages of the study. An initial pass used the Faiman default free-standing coefficients (U_c = 25.0 W/m²K, U_V = 6.84 W/m²K per m/s) with a literature-representative temperature coefficient of -0.35%/°C. Following cross validation against PVsyst 7.4.8 (Section 2.8), the coefficients were revised to match the as-installed system: U_c = 25.0 W/m²K, U_V = 6.5 W/m²K per m/s, and a temperature coefficient of -0.29%/$°C$ corresponding to the datasheet value of the AIKO (A625) MAH72Dw module actually specified for the reference project. All results reported in Section 3 use this revised, PVsyst-matched parameter set.

Annual thermal derating loss was calculated as the POA weighted difference between the actual power ratio and a no loss reference held at 25°C, restricted to daytime hours (POA > 5 W/m²):

$$Power\ ratio = 1 + \gamma(T_{cell} - 25)$$

where γ is the temperature coefficient of power. Weighting the loss by POA rather than averaging it over hours ensures that the reported percentage reflects the actual annual energy loss rather than the average temperature excursion.

2.4 Soiling Loss Model

No field soiling measurements were available for Libya. Daily soiling accumulation rates were therefore assigned to each zone from the wider body of MENA and Gulf soiling literature reviewed in Section 1, selecting rates consistent with each zone's dust exposure and coastal proximity: 0.18%/day for Zone A, 0.32%/day for Zone B, and 0.55%/day for Zone C. These rates are derived from comparable arid environments in the MENA/Gulf region and should be treated as estimates requiring local validation rather than measurements taken in Libya. Soiling was modeled as a linear ramp from zero at the last cleaning event to a peak set by the cleaning interval, capped at a 30% saturation level to reflect the self-limiting effect of wind removal and gravity at high dust loading. The average annual soiling loss was computed for cleaning intervals of 7, 14, 21, 30, 45, 60, 90, and 120 days in each zone.

Humidity-Based PID and Corrosion Risk Indicator

Potential-induced degradation (PID) and connector corrosion both accelerate under combined heat and humidity exposure. In the absence of a system-voltage-specific PID model, an ambient-based proxy was constructed for each station: the annual count of hours with relative humidity above 60% and air temperature above 25°C. The mean overnight dew-point margin (air temperature minus dew-point temperature) was also computed as a secondary indicator of condensation risk on the module surface.

Wind Effects

Wind was evaluated separately for its cooling contribution to cell temperature and for its structural design implications. The cooling contribution was isolated by re-running the Faiman model with wind speed fixed at a sheltered reference value of 1 m/s and comparing the resulting thermal loss to the loss obtained with the station's actual wind speed; the difference is reported as the wind-cooling benefit in percentage points of annual thermal loss recovered. Structural design exposure was characterized using the 99th-percentile wind speed and the annual maximum recorded gust at each station, since extreme, short-duration gust events determine mounting-structure design loads while the mean wind speed determines the cooling benefit.

Net Specific Yield

The net specific energy yield (kWh/kWp/year) for each zone was obtained by combining the POA irradiance with the thermal and soiling loss fractions and a fixed balance-of-system factor of 0.95, representing inverter, DC/AC wiring, and availability losses held constant across zones so that the comparison isolates climate-driven variation:

$$Net\ Yield = POA \times (1 - thermal\ loss) \times (1 - soiling\ loss) \times 0.95$$

Net yield was computed under two maintenance scenarios: a uniform 30-day cleaning cycle applied to all three zones, and a zone-appropriate cycle following the cleaning interval recommended in Section 3.6 for each zone (30-45 days for Zone A, 30 days for Zone B, 7-14 days for Zone C).

PVsyst Cross Validation

The pvlib-based results were cross-validated against PVsyst 7.4.8 using an existing 30 kWp grid-connected design (Project UNDP-Libya, Lot 01) simulated at three representative sites, one per zone: Tripoli (Zone A), Gharyan (Zone B), and Sabha (Zone C). All three simulations used an identical fixed-tilt array (32°/0°), the same AIKO-A625-MAH72Dw module and Huawei SUN2000-30KTL-M3 inverter, and the same thermal loss factor (Uc = 25.0 W/m²K, Uv = 6.5 W/m²K per m/s), so that geographic location was the only variable between runs. PVsyst's built-in Meteonorm weather data were used for these three runs rather than the TMYx files used elsewhere in the study, since PVsyst does not accept the TMYx format directly; the resulting difference in annual global horizontal irradiation (up to 11% between the two weather sources) is treated as a known limitation of the cross-validation and the comparison is restricted to loss percentages rather than absolute energy values. The soiling loss fraction obtained in Section 2.4 was entered directly into PVsyst's monthly soiling loss factor for the Gharyan and Sabha runs, providing an additional check on the soiling assumptions against an independently reported specific yield.

Results and discussion

Climate Zone Classification

The k-means clustering described in Section 2.2 separated the twelve stations into three zones with distinct climate signatures. Table 1 summarizes the range of each metric within each zone, and Fig. 1 shows the resulting spatial distribution.

Table 1 Data-driven climate zone characteristics.

Zone	Stations	Elevation (m)	Mean temperature (°C)	Mean RH (%)	GHI (kWh/m²/yr)
A (Coastal Mediterranean)	Tripoli, Zuwara, Derna, Misrata, Benghazi	3-132	19.8-21.5	62-68	1970-2008
B (Highland Transitional)	Gharyan, Yefran, Hamada	623-728	19.6-20.9	37-54	2046-2177
C (Desert Interior)	Ghadamis, Sabha, Awbari, Kufra	342-463	23.5-24.7	28-34	2179-2411

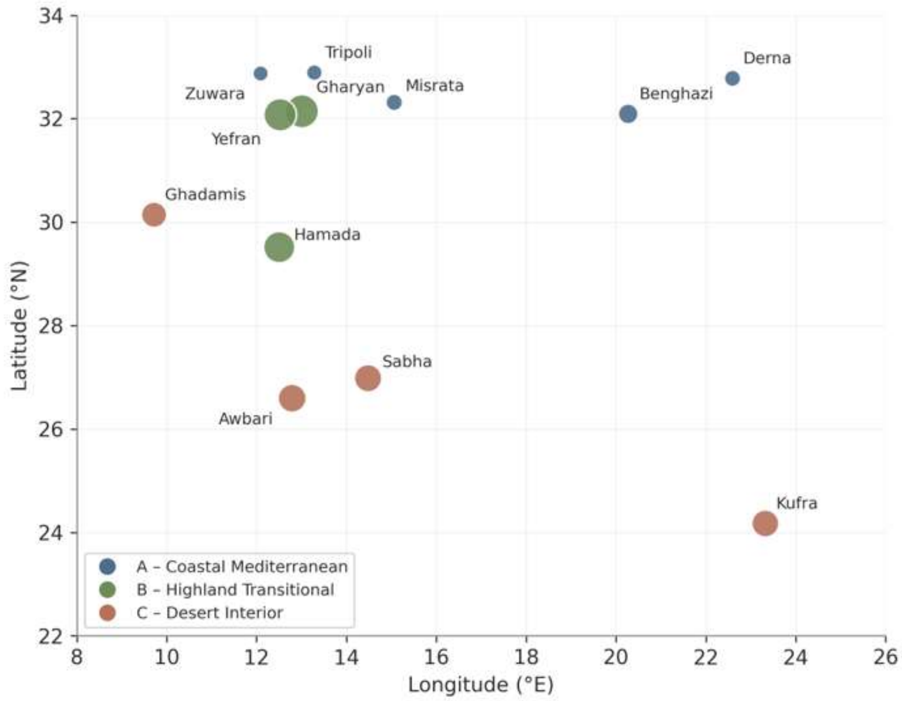

Figure 1: Spatial distribution of the twelve weather stations across Libya's three data-derived PV climate zones.

Zone A stations sit below 132 m and show the highest relative humidity of the three zones. Zone C stations show the highest irradiation and the lowest relative humidity. Zone B occupies an intermediate position in temperature and irradiation but the lowest relative humidity range once Hamada is included, since Hamada's 36.6% mean RH lies closer to the desert-interior range than to Gharyan or Yefran. Hamada was nonetheless retained in Zone B because its elevation (623 m) placed it there under the clustering algorithm, and it is treated as a transitional case in the results that follow.

Thermal Derating

Cell temperature and the resulting annual thermal derating loss were computed using the Faiman model with the PVsyst-matched parameters (U_c = 25.0 W/m²K, U_V = 6.5 W/m²K per m/s, γ = -0.29%/°C). Table 2 reports the results by zone, and Fig. 2 plots the thermal loss against the plane-of-array (POA) irradiance for each zone.

Table 2 Annual thermal derating by climate zone.

Zone	POA (kWh/m²/yr)	Mean daytime cell temperature (°C)	Maximum cell temperature (°C)	Annual thermal loss (%)
A (Coastal)	2189.6	32.3	70.3	3.39
B (Highland)	2290.0	34.8	78.2	4.36
C (Desert Interior)	2423.3	39.0	82.9	5.35

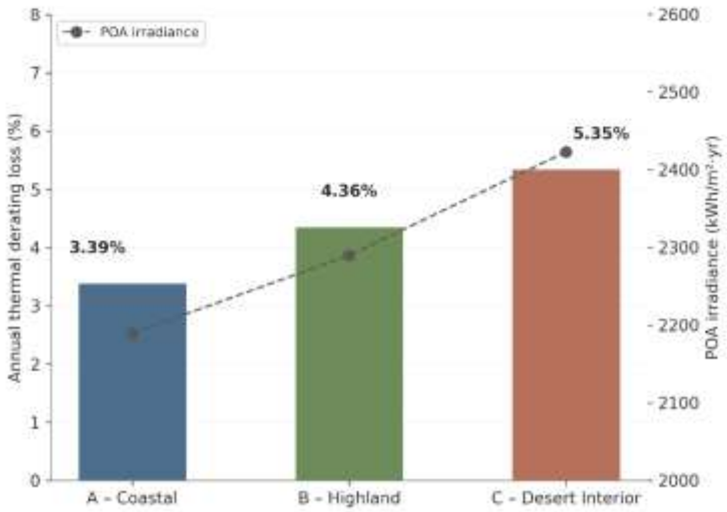

Figure 2: Annual thermal derating loss vs. plane of array irradiance by climate zone.

The thermal loss increases from 3.39% in Zone A to 5.35% in Zone C, a relative increase of 58% between the two zones. The POA irradiance increases by only 11% over the same range (2189.6 to 2423.3 kWh/m²/yr). Therefore, the additional irradiance available in the desert interior is partly offset by a disproportionately larger thermal loss, and the two effects do not cancel evenly across zones. Maximum cell temperature exceeds the recorded maximum air temperature at each station by more than 30°C, which confirms that ambient temperature alone would substantially underestimate the thermal stress experienced by the module surface.

Soiling Sensitivity

Table 3 and Fig. 3 report the average annual soiling loss for each zone across a range of cleaning intervals, using the literature-derived daily accumulation rates described in Section 2.4 (0.18, 0.32, and 0.55%/day for Zones A, B, and C).

Table 3 Average annual soiling loss (%) by cleaning interval.

Cleaning interval (days)	Zone A	Zone B	Zone C
7	0.63	1.12	1.93
14	1.26	2.24	3.85
30	2.70	4.80	8.25
60	5.40	9.60	16.36
90	8.10	14.40	20.91
120	10.80	18.28	23.18

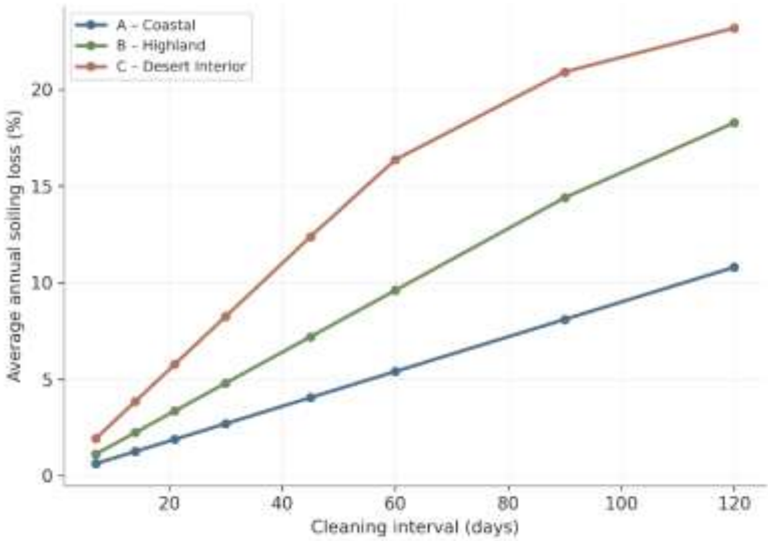

Figure 3: Soiling-induced energy loss vs. cleaning interval by climate zone.

At a 7-day cleaning interval, the gap between Zone A and Zone C is 1.30% points (0.63% vs. 1.93%). At a 30-day interval, the gap widens to 5.55% points (2.70% vs. 8.25%), and at 90 days it reaches 12.81% points. The soiling penalty for infrequent cleaning therefore grows faster than linearly with the difference in dust exposure between zones, which means a single national cleaning schedule imposes a much larger relative cost on Zone C than on Zone A.

Humidity-Based PID and Corrosion Risk

Table 4 reports the annual combined heat-humidity stress hours (relative humidity above 60% and air temperature above 25°C) and the mean overnight dew-point margin for each zone. Fig. 4 plots the stress-hour values on a logarithmic scale, since the range spans nearly three orders of magnitude.

Table 4 Humidity-based PID and corrosion risk indicators.

Zone	Combined heat-humidity stress (h/yr)	Mean dew-point margin (°C)
A (Coastal)	1119.8	7.5
B (Highland)	77.7	13.4
C (Desert Interior)	2.8	20.7

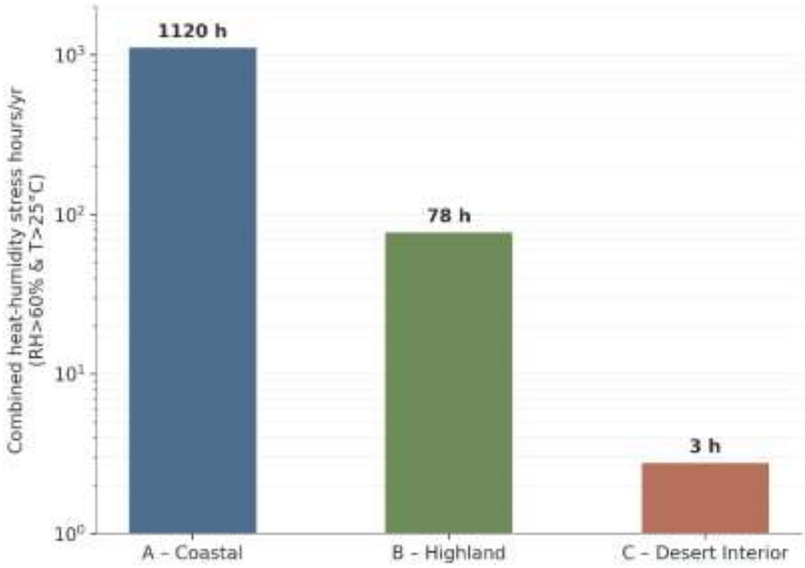

Figure 4: Annual combined heat-humidity stress hours by zone (log scale).

Zone A records 1119.8 stress hours per year, compared with 77.7 in Zone B and 2.8 in Zone C. The stress hours in Zone A therefore exceed those in Zone C by a factor of about 400. The dew-point margin follows the same ordering in reverse, from 7.5°C in Zone A to 20.7°C in Zone C, which indicates a substantially higher likelihood of nighttime condensation on module surfaces in the coastal zone. On this basis, humidity-driven degradation risk in Libya is concentrated almost entirely in the coastal zone rather than distributed evenly across the country. This indicator is a hypothesized proxy; outdoor exposure or accelerated PID testing is needed to confirm the degradation risk.

Wind Effects

Wind was evaluated for its cooling contribution and its structural design implications, as described in Section 2.6. Table 5 reports both measures alongside the mean wind speed for each zone; Fig. 5 shows the same data graphically.

Table 5 Wind cooling contribution and structural design indicators.

Zone	Mean wind speed (m/s)	Wind-cooling benefit (pct. pts. of thermal loss recovered)	Annual maximum gust (m/s)
A (Coastal)	4.64	2.78	30.9
B (Highland)	3.66	2.15	16.5
C (Desert Interior)	3.96	2.54	40.0

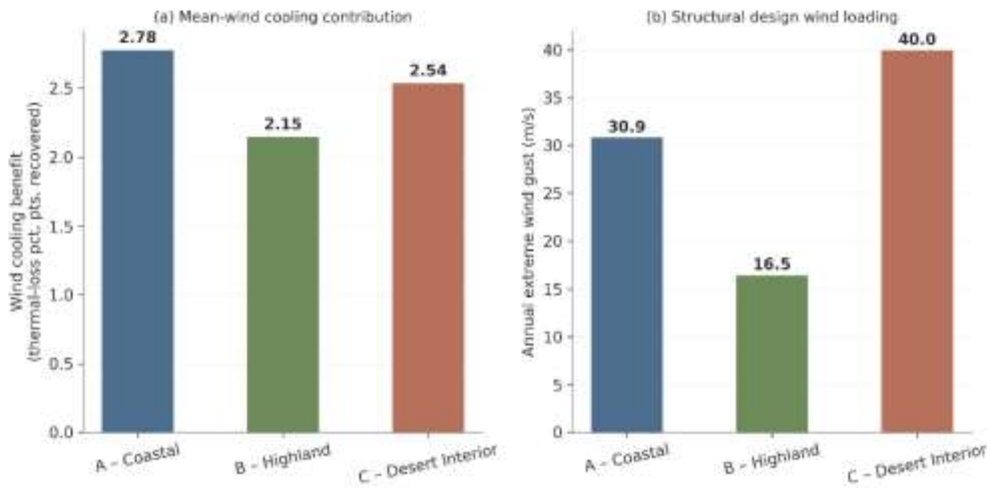

Figure 5: Wind effects on PV performance and structural design by zone.

Zone A has the highest mean wind speed (4.64 m/s) and the largest wind-cooling benefit (2.78 percentage points of thermal loss recovered). Zone C records the highest annual maximum gust (40.0 m/s, at Awbari) despite a mean wind speed lower than Zone A's. This combination, a comparatively low annual mean with an extreme short-duration maximum, is consistent with transient dust-storm events rather than persistent high wind. Consequently, mounting-structure design in Zone C should be based on the recorded gust maximum rather than the mean wind speed, while the cell-cooling benefit used in Section 3.2 is correctly based on the mean.

Combined Multi-Stress Profile

Fig. 6 combines the four stress dimensions, thermal loss, soiling loss at a 30-day cleaning cycle, humidity stress hours, and extreme gust, into a single normalized radar plot, with each axis scaled from 0 to 1 across the three zones. Zone C occupies the largest area on the thermal, soiling, and gust axes. Zone A occupies the largest area on the humidity axis and the smallest area on the other three. Zone B falls between the two on every axis except humidity, where it sits closer to Zone C. No zone is subject to all four stresses simultaneously, which is the basis for the zone-specific specification approach developed in Section 3.8 rather than a single national specification.

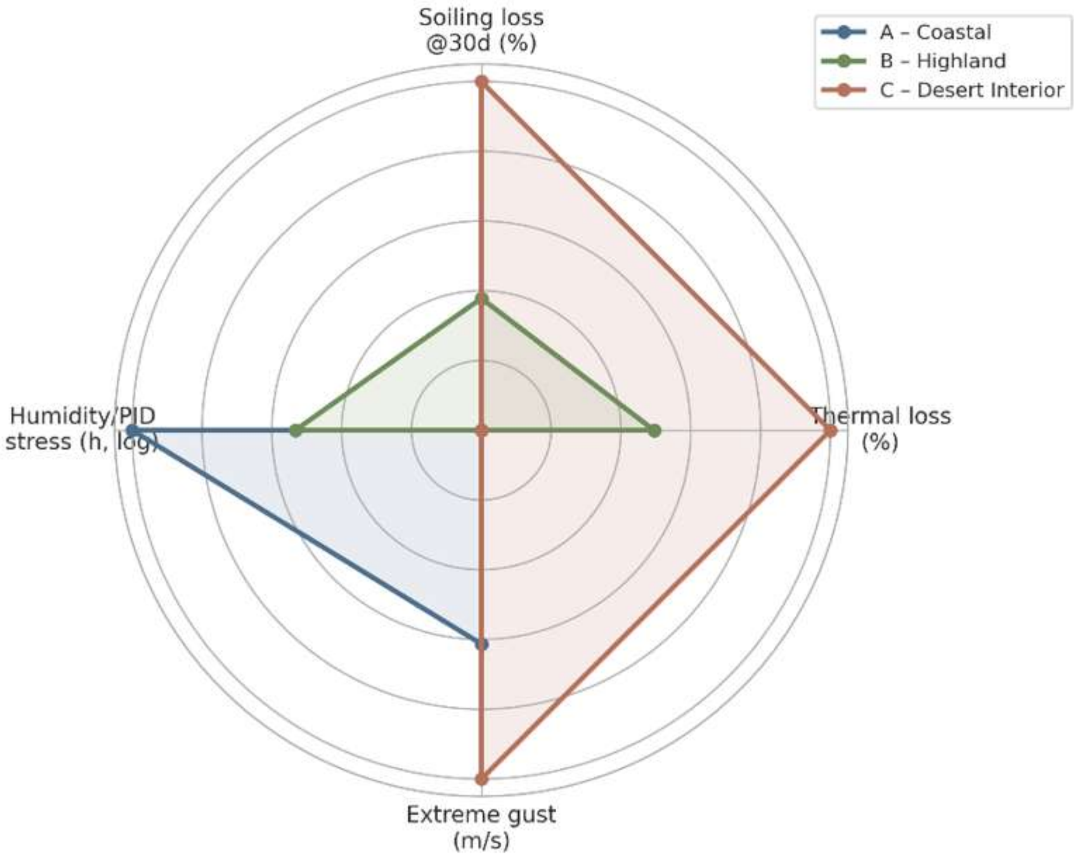

Figure 6: Normalized multi-stress climate profile by PV climate zone.

Net Specific Energy Yield

Table 6 reports the net specific energy yield (kWh/kWp/yr), combining the POA irradiance, thermal loss, and soiling loss as described in Section 2.7, under two maintenance scenarios: a uniform 30-day cleaning cycle applied to all zones, and a zone-appropriate cleaning cycle following the recommendation given in Section 3.8. Fig. 7 shows both scenarios side by side.

Table 6 Net specific energy yield under uniform and zone-appropriate maintenance.

Zone	Net yield, uniform 30 day cleaning (kWh/kWp/yr)	Net yield, zone-appropriate cleaning (kWh/kWp/yr)	Recommended cleaning interval (days)
A (Coastal)	1955	1955	30
B (Highland)	1981	1981	30
C (Desert Interior)	1999	2095	14

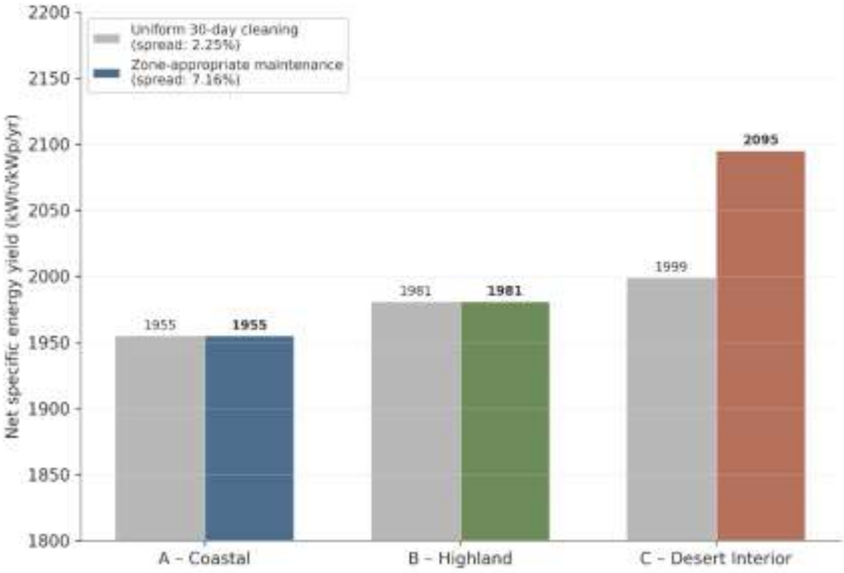

Figure 7: Net PV energy yield by climate zone: uniform vs. zone-appropriate maintenance schedule.

Under uniform 30-day cleaning, the spread between the highest- and lowest-yielding zone is 1955 to 1999 kWh/kWp/yr, a difference of 2.25%. Under zone-appropriate cleaning, Zone C's yield increases from 1999 to 2095 kWh/kWp/yr, and the spread widens to 7.16%. This result indicates that Libya's climate zones do not differ greatly in raw solar energy potential once thermal and soiling losses are accounted for under a common maintenance regime. What differs substantially is the maintenance investment required to realize that potential, and a uniform national maintenance schedule leaves part of the desert interior's higher irradiance unused.

Zone-Specific Specification Matrix

The results of Sections 3.2 to 3.7 were combined into a specification matrix (Table 7, shown graphically in Fig. 8) that recommends a module technology, PID mitigation measure, frame corrosion class, cleaning cycle, and structural wind rating for each zone.

Table 7 Zone-specific PV module and system specification matrix.

Specification	Zone A - Coastal	Zone B - Highland	Zone C - Desert Interior
Dominant stress	Humidity/corrosion (1119.8 h/yr)	Balanced across factors	Heat, soiling, and gust (5.35% thermal, 0.55%/day soiling)
Cell technology	AIKO ABC or equivalent (γ ≈ -0.29%/°C)	Same as Zone A	Lower-γ technology preferred (e.g., HJT, γ ≈ -0.26%/°C)
PID mitigation	PID-resistant n-type cells or anti-PID p-type with premium EVA	Standard encapsulation	Standard encapsulation
Frame/corrosion class	Marine-grade anodized aluminum, C4-C5 coating	Standard anodized aluminum	Standard coating with UV-stabilized polymer components
Cleaning cycle	30-45 days	30 days	7-14 days, with anti-soiling coating or robotic cleaning
Structural wind design	≥31 m/s gust	Standard loading	≥40 m/s gust, reinforced anchoring

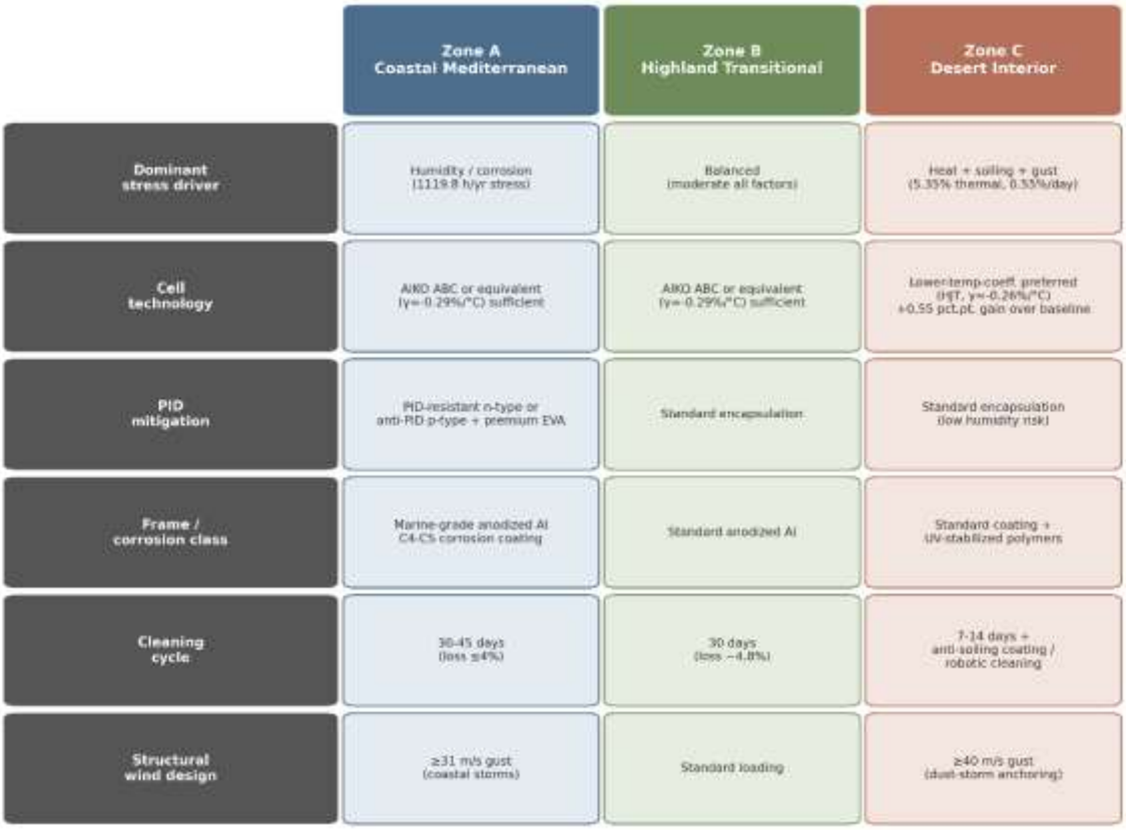

Figure 8: PV module and system specification decision matrix by Libyan climate zone.

The dominant stress differs by zone: Zone A is limited primarily by humidity-related degradation risk and coastal corrosion, Zone C by the combination of thermal loss, soiling, and extreme wind gust, and Zone B by a more even mix of all four factors. The cell-technology comparison in Section 3.9 shows that switching from the AIKO ABC baseline to a lower-temperature-coefficient technology in Zone C recovers a further 0.55 percentage points of thermal loss, which is a smaller margin than would be expected from a generic mono-PERC baseline, since the AIKO ABC module's own temperature coefficient (-0.29%/°C) already performs close to the TOPCon reference value (-0.30%/°C) used in that comparison.

Cell Technology Comparison in Zone C

Because Zone C carries the largest thermal penalty, an additional comparison isolated the effect of cell temperature coefficient alone, holding the thermal environment (POA, ambient temperature, wind speed) constant across three technologies: the as-installed AIKO ABC module (γ = -0.29%/°C), a representative n-type TOPCon module (γ = -0.30%/°C), and a representative heterojunction (HJT) module (γ = -0.26%/°C). Table 8 reports the resulting thermal loss at each of the four Zone C stations; Fig. 9 shows the same comparison graphically.

Table 8 Thermal derating loss by cell technology in Zone C.

Station	AIKO ABC (γ=-0.29%)	TOPCon (γ=-0.30%)	HJT (γ=-0.26%)
Ghadamis	5.13	5.31	4.60
Sabha	5.04	5.21	4.52
Awbari	5.43	5.62	4.87
Kufra	5.80	6.00	5.20
Zone C average	5.35	5.54	4.80

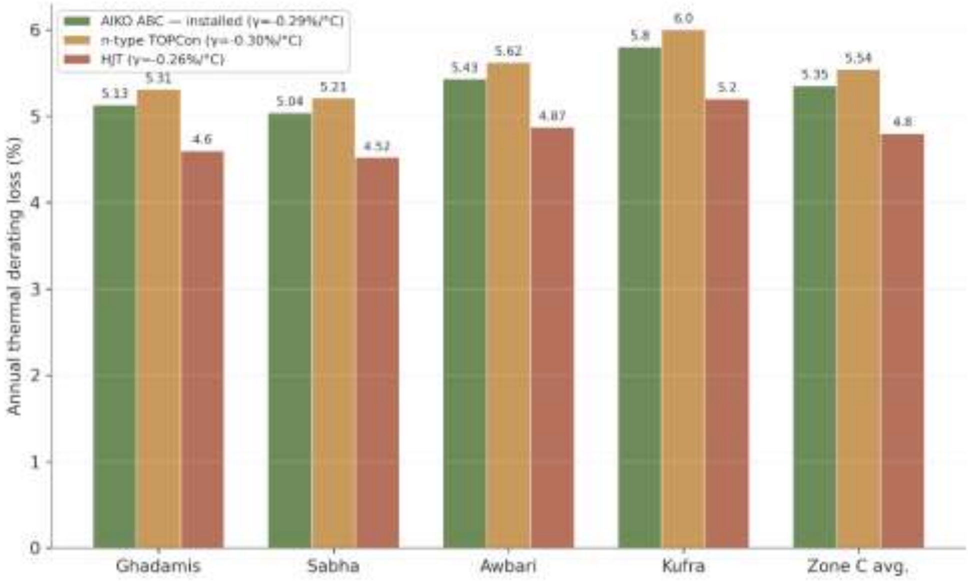

Figure 9: Cell-technology comparison of annual thermal derating loss in Zone C.

The AIKO ABC module already outperforms the representative TOPCon module by 0.19 percentage points on average (5.35% vs. 5.54%), which confirms that the module actually specified for the reference project is a reasonable choice for the desert interior zone even without switching technology. The HJT comparison shows a further 0.55 percentage point reduction relative to the AIKO ABC baseline (5.35% to 4.80%), corresponding to an estimated 0.55-0.60% gain in annual energy yield from thermal derating alone if HJT modules were substituted in Zone C.

PVsyst Cross Validation

Validation Setup

The pvlib-based results in Section 3 were checked against PVsyst 7.4.8 using an existing 30 kWp grid-connected design simulated at three sites, one representative of each zone: Tripoli (Zone A), Gharyan (Zone B), and Sabha (Zone C). All three simulations used the same fixed tilt array orientation (32°/0°), the same AIKO-A625-MAH72Dw module and Huawei SUN2000-30KTL-M3 inverter, and the same thermal loss factor (U_c = 25.0 W/m²K, U_V = 6.5 W/m²K per m/s), so that geographic location was the only variable between runs.

Thermal Loss Comparison

Table 9 compares the annual thermal derating loss computed by pvlib and by PVsyst at each of the three stations, using identical U_c, U_V, and γ values in both tools. Fig. 10 shows the same comparison graphically, together with the gap between the two tools at each station.

Table 9 PVlib vs. PVsyst thermal derating loss, identical U_c=25.0, U_V=6.5, γ=-0.29%/°C.

Station (zone)	pvlib thermal loss (%)	PVsyst thermal loss (%)	Gap (percentage points)
Tripoli (A)	3.67	2.44	1.23
Gharyan (B)	4.04	2.69	1.35
Sabha (C)	4.99	3.12	1.87

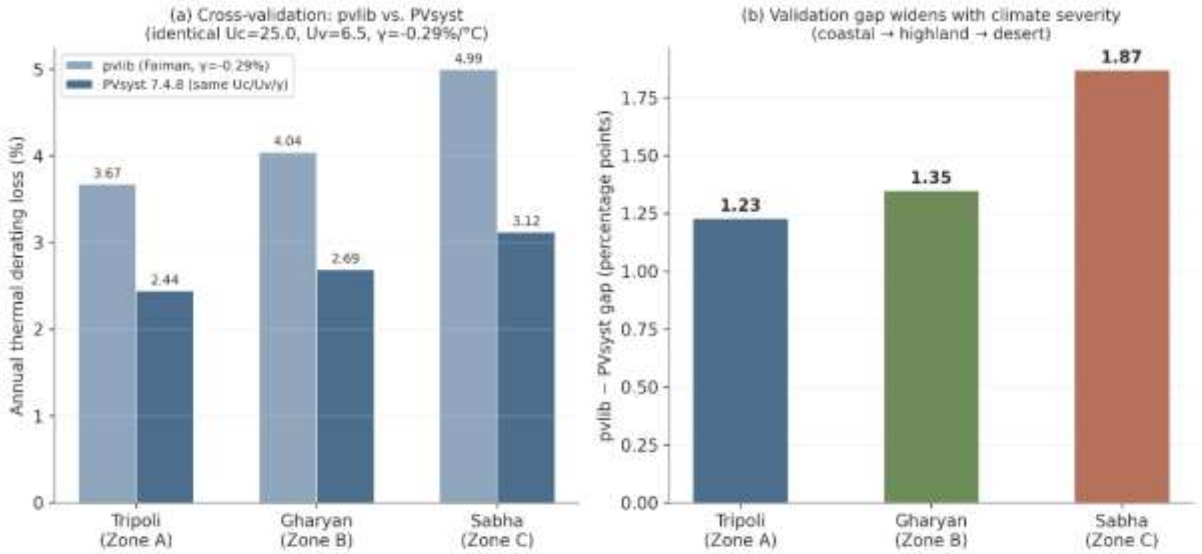

Figure 10: Cross-validation of the pvlib/Faiman thermal model against PVsyst 7.4.8.

PVsyst consistently reports a lower thermal loss than pvlib at every station, and the gap widens from 1.23 percentage points in Tripoli to 1.87 percentage points in Sabha. The gap therefore increases with climate severity rather than remaining constant, which indicates a systematic difference in how the two tools reference the thermal loss rather than a random discrepancy. The most likely source is a difference in the two tools' internal accounting: PVsyst reports "PV loss due to temperature" as one line in a loss diagram computed relative to an STC-efficiency reference derived from IAM-corrected effective irradiance, while the pvlib calculation in Section 2.3 compares POA-weighted actual power directly to a no-loss reference at the same POA. Both values are reported here rather than treated as interchangeable, since neither tool's internal accounting convention can be assumed to be the ground truth for the other.

Soiling and Net Yield Cross-Check

The soiling loss fractions derived in Section 2.4 (4.80% for Zone B, 8.25% for Zone C, at a 30-day cleaning cycle) were entered directly into PVsyst's monthly soiling loss factor for the Gharyan and Sabha runs. PVsyst reported soiling losses of 4.8% for Gharyan and 8.3% for Sabha, matching the entered values to within rounding, which confirms that the values were transferred correctly and provides no independent check on the soiling rate itself, since the same number was supplied as an input.

A more informative check is available from PVsyst's own specific yield, which reflects the combined effect of irradiance, thermal loss, soiling, and system losses rather than a single input value. Table 10 reports the specific yield from the three PVsyst runs, each using its own zone-appropriate soiling input.

Table 10 PVsyst specific yield by station, zone-appropriate soiling input.

Station (zone)	Soiling input (%)	Specific yield (kWh/kWp/yr)
Tripoli (A)	0.0	1791
Gharyan (B)	4.8	1775
Sabha (C)	8.3	1889

Despite carrying the highest thermal loss and the highest soiling loss of the three stations, Sabha produces the highest specific yield (1889 kWh/kWp/yr), exceeding Gharyan by 6.4% and Tripoli by 5.5%. This result, obtained independently from an industry-standard commercial simulation tool rather than from the pvlib-based model, corroborates the net-yield finding reported in Section 3.7: Libya's desert interior does not underperform the coastal and highland zones once its higher irradiance is accounted for, and can outperform them despite its larger thermal and soiling penalties.

The cross validation produced two results. First, the two independent tools disagree on the absolute thermal loss percentage by 1.2 to 1.9 percentage points, with the disagreement growing systematically from the coastal to the desert-interior zone; this gap is reported as a methodological limitation rather than resolved in favor of either tool. Second, and more directly relevant to the paper's central claim, PVsyst's own specific-yield output confirms, independently of the pvlib based model, that the desert-interior zone yields more energy per installed kilowatt-peak than the coastal or highland zones under realistic soiling conditions. The second result is considered the stronger validation outcome, since it was not built into the PVsyst simulation as an assumption but emerged from PVsyst's own calculation.

Conclusion

The Libya specific literature reviewed in Section 1 has established that PV performance varies across the country and that module selection should account for this variation, but each study covers a single site or a single stress factor. Nassar et al. [4,5] mapped suitable module and inverter types across Libyan territory using Solargis data and SAM simulations, and reported savings of up to 45% from matching module type to location; that result motivates the present study but does not itself integrate thermal, soiling, humidity, and wind effects into one framework, nor does it derive its climate zones directly from station-level weather data. The present study closes that gap by combining four stress factors that are normally studied separately, over a station-based climate zoning derived statistically from the same twelve stations used in the performance analysis, and by expressing the result as a specification matrix (Table 7) rather than a performance map alone.

The soiling literature is extensive across the Gulf and the wider MENA region [19,33-53], and the thermal-modeling literature is well developed for desert and semi-arid climates in general [15-24]. Neither body of work has previously been applied together to Libya, and neither has been combined with a humidity-based PID and corrosion risk indicator of the kind constructed in Section 2.5. The result in Section 3.4, that combined heat-humidity stress hours in the coastal zone exceed those in the desert interior by a factor of about 400, is, to the authors' knowledge, the first quantification of this contrast for Libya specifically, and it directly supports a design recommendation (PID-resistant cells and marine-grade corrosion coatings in Zone A only) that a single national specification would not produce.

A key contribution of the study is the distinction, established in Section 3.7, between raw solar potential and realized energy yield under maintenance constraints. Under a uniform 30-day cleaning cycle, the three zones differ by only 2.25% in net specific yield (Table 6), which would suggest that geographic location has a limited effect on PV output in Libya. Under a zone-appropriate cleaning schedule, the same comparison widens to 7.16%, entirely because the desert interior's higher irradiance is realized only when its soiling is managed at the shorter interval the zone requires. This finding reframes the research question posed in the paper's title: climate zone in Libya does not primarily determine how much energy a well-specified and well-maintained PV system can produce, but rather what specification and maintenance investment are required to produce it. The cross-validation in Section 4.3, where PVsyst's own specific yield output independently reproduces the same ordering (Sabha outproducing Tripoli and Gharyan despite higher losses), was obtained from a commercial tool without this finding built in as an input, which strengthens confidence that the result is not an artifact of the pvlib based model alone.

The three limitations most likely to affect how these results are used are addressed first: the soiling rates, the PID risk indicator, and the absence of an economic analysis.

The soiling model in Section 2.4 uses daily accumulation rates of 0.18, 0.32, and 0.55%/day for Zones A, B, and C, drawn from soiling studies in comparable arid environments rather than from measurements taken in Libya. These rates are derived from comparable arid environments in the MENA/Gulf region and should be treated as estimates requiring local validation rather than measurements taken in Libya. The resulting soiling losses in Table 3 should therefore be read as a sensitivity scenario rather than a validated estimate. Field soiling stations at a representative site in each zone are needed to calibrate the daily rate and the 30% saturation cap used in the model.

The humidity-based indicator in Section 3.4 is an ambient-air proxy for PID and corrosion risk, not a measured degradation rate. PID severity also depends on system voltage architecture and grounding configuration, which are not included here. This indicator is a hypothesized proxy; outdoor exposure or accelerated PID testing is needed to confirm the degradation risk. The indicator is strong enough to justify differentiated encapsulation and frame corrosion class by zone, but it cannot replace outdoor exposure testing or accelerated PID testing on modules representative of the Libyan market.

No economic analysis is included. The specification upgrades in Table 7, marine-grade coatings and PID resistant cells in Zone A, lower-γ cells and more frequent cleaning in Zone C, all carry a cost premium that is not quantified here against the energy value recovered. A levelized cost of energy comparison across the three zones would determine whether each recommended upgrade is economically justified and not only technically beneficial.

Future work should prioritize four items. (1) Installation of soiling monitoring stations in at least one site per zone to replace the literature-derived deposition rates with measured ones. (2) Outdoor or accelerated PID testing on modules representative of the Libyan market, under the humidity and temperature combinations identified in Section 3.4. (3) A levelized cost of energy analysis combining the specification upgrades proposed here with representative component and installation costs in Libya. (4) Comparison of the TMYx extreme wind values against long-term meteorological records or national wind hazard data to set a defensible design wind speed for each zone.

Compliance with ethical standards

Disclosure of conflict of interest

The authors declare that they have no conflict of interest.

References

[1] Y. Kassem, H. Çamur, and R. A. F. Aateg, "Exploring Solar and Wind Energy as a Power Generation Source for Solving the Electricity Crisis in Libya," *Energies (Basel).*, vol. 13, p. 3708, 2020, doi: 10.3390/en13143708.
[2] Y. Nassar *et al.*, "Solar and Wind Atlas for Libya," *International Journal of Electrical Engineering and Sustainability*, p., 2023, doi: 10.65998/ijees.v1i3.44.
[3] Y. Nassar and A. Salem, "The reliability of the photovoltaic utilization in southern cities of Libya," *Desalination*, vol. 209, pp. 86–90, 2007, doi: 10.1016/j.desal.2007.04.013.
[4] Y. Nassar, H. El-Khozondar, S. Alsadi, N. Abuhamoud, and G. Miskeen, "Atlas of PV Solar Systems Across Libyan Territory," in *2022 International Conference on Engineering & MIS (ICEMIS)*, 2022, pp. 1–6. doi: 10.1109/icemis56295.2022.9914355.
[5] Y. Nassar, S. Alsadi, G. Miskeen, H. El-Khozondar, and N. Abuhamoud, "Mapping of PV Solar Module Technologies Across Libyan Territory," in *2022 Iraqi International Conference on Communication and Information Technologies (IICCIT)*, 2022, pp. 227–232. doi: 10.1109/iiccit55816.2022.10010476.
[6] I. H. Tawil and Z. A. Gebrel, "Thermal Performance Challenges and Mitigation Strategies for Photovoltaic Modules in High-Temperature Climates: A Case Study of Three Libyan Cities in Different Regions," *Al-imad Journal of Humanities and Applied Sciences*, p., 2026, doi: 10.64943/ajhas.2026.020119.
[7] A. S. A. S. Moodu, "Performance Evaluation of a 2 MW On-grid Solar Photovoltaic Plant with Single-Axis Tracker in the Hyper-Arid Climate of Traghn, South Libya," *International Journal For Multidisciplinary Research*, p., 2025, doi: 10.36948/ijfmr.2025.v07i06.64101.
[8] "Geoclimatic Analysis of the Performance of 500-Watt Photovoltaic Solar Panels in Qasr Bin Ghashir, Libya," *Alqalam Journal of Science*, p., 2025, doi: 10.69667/ajs.25203.
[9] A. Alsharif, "Mitigation of Dust Impact on Solar Photovoltaics Performance Considering Libyan Climate Zone: A Review," *Engineering Technology Open Access Journal*, p., 2023, doi: 10.19080/etoaj.2023.05.555662.
[10] A. Elbaz and A. Elfaqih, "Impact of Dust Accumulation on Photovoltaic System Performance in a Coast Environment-Case Study in Libya," in *2023 IEEE 11th International Conference on Systems and Control (ICSC)*, 2023, pp. 959–963. doi: 10.1109/icsc58660.2023.10449762.
[11] J. Ascencio-Vásquez, K. Brecl, and M. Topič, "Methodology of Köppen-Geiger-Photovoltaic climate classification and implications to worldwide mapping of PV system performance," *Solar Energy*, p., 2019, doi: 10.1016/j.solener.2019.08.072.
[12] T. Huld and A. Amillo, "Estimating PV Module Performance over Large Geographical Regions: The Role of Irradiance, Air Temperature, Wind Speed and Solar Spectrum," *Energies (Basel).*, vol. 8, pp. 1–23, 2015, doi: 10.3390/en8065159.
[13] O. Bamisile, C. Acen, D. Cai, Q. Huang, and I. Staffell, "The environmental factors affecting solar photovoltaic output," *Renewable and Sustainable Energy Reviews*, p., 2025, doi: 10.1016/j.rser.2024.115073.
[14] B. Adothu *et al.*, "Comprehensive review on performance, reliability, and roadmap of c-Si PV modules in desert climates: A proposal for improved testing standard," *Progress in Photovoltaics: Research and Applications*, vol. 32, pp. 495–527, 2024, doi: 10.1002/pip.3827.

[15] M. Kempe, D. Holsapple, K. Whitfield, and N. Shiradkar, “Standards development for modules in high temperature micro-environments,” *Progress in Photovoltaics: Research and Applications*, vol. 29, pp. 445–460, 2021, doi: 10.1002/pip.3389.
[16] W. Herrmann, G. Bardizza, G. Friesen, S. Riechelmann, and H. Müllejans, “Uncertainty of Climate Specific Energy Rating (CSER) of PV Modules in Accordance With IEC 61853,” *Progress in Photovoltaics: Research and Applications*, vol. 33, pp. 1124–1138, 2025, doi: 10.1002/pip.70007.
[17] C. Monokroussos *et al.*, “Energy performance of commercial c-Si PV modules in accordance with IEC 61853-1, -2 and impact on the annual specific yield,” *EPJ Photovoltaics*, p., 2023, doi: 10.1051/epjpv/2022032.
[18] A. Kirsten Vidal de Oliveira, M. Braga, H. Naspolini, and R. Rüther, “Validation of Thermal Models for Bifacial Photovoltaic Systems Under Various Albedo Conditions,” *Progress in Photovoltaics: Research and Applications*, vol. 34, pp. 103–184, 2025, doi: 10.1002/pip.3892.
[19] F. Nyarko, G. Takyi, E. Amalu, and M. Adaramola, “Generating temperature cycle profile from in-situ climatic condition for accurate prediction of thermo-mechanical degradation of c-Si photovoltaic module,” *Engineering Science and Technology, an International Journal*, p., 2019, doi: 10.1016/j.jestch.2018.12.007.
[20] P. Bevilacqua, S. Perrella, R. Bruno, and N. Arcuri, “An accurate thermal model for the PV electric generation prediction: long-term validation in different climatic conditions,” *Renew. Energy*, vol. 163, pp. 1092–1112, 2020, doi: 10.1016/j.renene.2020.07.115.
[21] M. Elyaqouti, N. Boulfaf, N. Hamid, D. Izbaim, J. Chaoufi, and L. Bouhouch, “Thermal and electrical modelling of photovoltaic modules,” *International Journal of Ambient Energy*, vol. 43, pp. 5793–5809, 2021, doi: 10.1080/01430750.2021.1994464.
[22] B. Jaeckel, D. Daßler, M. Pander, J. John, S. Kumar, and B. Adothu, “Mission profile concept for PV modules: use case – middle east deserts vs temperate European climate,” *EPJ Photovoltaics*, p., 2023, doi: 10.1051/epjpv/2023030.
[23] I. Lamaamar, A. Tilioua, Z. Ben Zaid, A. Babaoui, M. Ettakni, and M. H. Alaoui, “Evaluation of different models for validating of photovoltaic cell temperature under semi-arid conditions,” *Heliyon*, vol. 7, p., 2021, doi: 10.1016/j.heliyon.2021.e08534.
[24] N. Aoun, “Outdoor testing of free standing PV module temperature under desert climate: a comparative study,” *International Journal of Ambient Energy*, vol. 42, pp. 1484–1491, 2019, doi: 10.1080/01430750.2019.1611640.
[25] M. Memiche, C. Bouzian, A. Benzahia, and A. Moussi, “Effects of dust, soiling, aging, and weather conditions on photovoltaic system performances in a Saharan environment—Case study in Algeria,” vol. 3, pp. 60–67, 2020, doi: 10.1016/j.gloei.2020.03.004.
[26] R. Dabou *et al.*, “Monitoring and performance analysis of grid connected photovoltaic under different climatic conditions in south Algeria,” *Energy Convers. Manag.*, vol. 130, pp. 200–206, 2016, doi: 10.1016/j.enconman.2016.10.058.
[27] S. Chabachi, N. Ammar, O. Abdelkhalek, A. Bouraiou, A. Ziane, and M. Hamouda, “Performance analysis of an experimental and simulated grid connected photovoltaic system in southwest Algeria,” *International Journal of Energy and Environmental Engineering*, vol. 13, pp. 831–851, 2022, doi: 10.1007/s40095-022-00474-9.
[28] A. Azouzoute *et al.*, “Modeling and experimental investigation of dust effect on glass cover PV module with fixed and tracking system under semi-arid climate,” *Solar Energy Materials and Solar Cells*, vol. 230, p. 111219, 2021, doi: 10.1016/j.solmat.2021.111219.
[29] A. A. Ali, Y. Ouhassan, M. Abouyaakoub, M. Chahboun, and H. Hihi, “The Impact of Desert Regions on Solar Energy Production with the Evaluation of Groundwater for Maintenance: A Case Study in Morocco,” *Sustainability*, p., 2024, doi: 10.3390/su16135476.
[30] B. Belmahdi and A. Bouardi, “Solar Potential Assessment using PVsyst Software in the Northern Zone of Morocco,” *Procedia Manuf.*, vol. 46, pp. 738–745, 2020, doi: 10.1016/j.promfg.2020.03.104.
[31] O. A. Omar, E. Fadil, N. E. El Fezazi, Z. Oumimoun, A. A. Errouhi, and O. Choukai, “Real yields and PVSYST simulations: comparative analysis based on four photovoltaic installations at Ibn Tofail University,” *Energy Harvesting and Systems*, vol. 11, p., 2023, doi: 10.1515/ehs-2023-0064.
[32] M. Abraim *et al.*, “Comparative Study of Soiling Effect on CSP and PV Technologies under Semi-arid Climate in Morocco,” *Solar Energy Advances*, p., 2022, doi: 10.1016/j.seja.2022.100021.
[33] B. Guo, W. Javed, B. Figgis, and T. Mirza, “Effect of dust and weather conditions on photovoltaic performance in Doha, Qatar,” *2015 First Workshop on Smart Grid and Renewable Energy (SGRE)*, pp. 1–6, 2015, doi: 10.1109/sgre.2015.7208718.
[34] W. Javed, B. Guo, B. Figgis, L. M. Pomares, and B. Aïssa, “Multi-year field assessment of seasonal variability of photovoltaic soiling and environmental factors in a desert environment,” *Solar Energy*, vol. 211, pp. 1392–1402, 2020, doi: 10.1016/j.solener.2020.10.076.

[35] B. Aïssa, R. Isaifan, V. Madhavan, and A. Abdallah, "Structural and physical properties of the dust particles in Qatar and their influence on the PV panel performance," *Sci. Rep.*, vol. 6, p., 2016, doi: 10.1038/srep31467.
[36] F. Touati, M. Al-Hitmi, and H. Bouchech, "Study of the Effects of Dust, Relative Humidity, and Temperature on Solar PV Performance in Doha: Comparison Between Monocrystalline and Amorphous PVS," *Int. J. Green Energy*, vol. 10, pp. 680–689, 2013, doi: 10.1080/15435075.2012.692134.
[37] F. Touati, A. Massoud, J. Hamad, and S. Saeed, "Effects of Environmental and Climatic Conditions on PV Efficiency in Qatar," *Renewable energy & power quality journal*, pp. 262–267, 2013, doi: 10.24084/repqj11.275.
[38] S. Jain, M. Abdelrahim, A. Abdallah, D. Pillai, and S. Bayhan, "Performance Modeling of Rooftop PV Systems in Arid Climate, a Case Study for Qatar: Impact of Soiling Losses and Albedo Using PVsyst and SAM," *Energies (Basel).*, p., 2025, doi: 10.3390/en18225876.
[39] A. Hachicha, I. Al-Sawafta, and Z. Said, "Impact of dust on the performance of solar photovoltaic (PV) systems under United Arab Emirates weather conditions," *Renew. Energy*, p., 2019, doi: 10.1016/j.renene.2019.04.004.
[40] H. Al Garni, "The Impact of Soiling on PV Module Performance in Saudi Arabia," *Energies (Basel).*, p., 2022, doi: 10.3390/en15218033.
[41] M. Adouane, A. Al-Qattan, B. Alabdulrazzaq, and A. Fakhraldeen, "Comparative performance evaluation of different photovoltaic modules technologies under Kuwait harsh climatic conditions," *Energy Reports*, p., 2020, doi: 10.1016/j.egyr.2020.09.034.
[42] I. Al Siyabi, A. Al Mayasi, A. Al Shukaili, and S. Khanna, "Effect of Soiling on Solar Photovoltaic Performance under Desert Climatic Conditions," *Energies (Basel).*, p., 2021, doi: 10.3390/en14030659.
[43] G. Chala, S. Sulaiman, and S. Al Alshaikh, "Effects of climatic conditions of Al Seeb in Oman on the performance of solar photovoltaic panels," *Heliyon*, vol. 10, p., 2024, doi: 10.1016/j.heliyon.2024.e30944.
[44] M. Chaichan *et al.*, "Sand and Dust Storms' Impact on the Efficiency of the Photovoltaic Modules Installed in Baghdad: A Review Study with an Empirical Investigation," *Energies (Basel).*, p., 2023, doi: 10.3390/en16093938.
[45] M. Hameed, I. Kaaya, M. Al-Jbori, Q. Matti, R. Scheer, and R. Gottschalg, "Analysis and Prediction of the Performance and Reliability of PV Modules installed in harsh climates: Case study Iraq," *Renew. Energy*, p., 2024, doi: 10.1016/j.renene.2024.120577.
[46] R. Othman and T. Hatem, "Assessment of PV technologies outdoor performance and commercial software estimation in hot and dry climates," *J. Clean. Prod.*, p., 2022, doi: 10.1016/j.jclepro.2022.130819.
[47] Y. Chanchangi, A. Ghosh, H. Baig, S. Sundaram, and T. Mallick, "Soiling on PV performance influenced by weather parameters in Northern Nigeria," *Renew. Energy*, p., 2021, doi: 10.1016/j.renene.2021.08.090.
[48] M. P. Ndeto, D. W. Wekesa, F. Njoka, and R. Kinyua, "Correlating dust deposits with wind speeds and relative humidity to overall performance of crystalline silicon solar cells: An experimental study of Machakos County, Kenya," *Solar Energy*, p., 2022, doi: 10.1016/j.solener.2022.09.050.
[49] H. Salimi, A. M. Lavasani, H. Ahmadi-Danesh-Ashtiani, and R. Fazaeli, "Effect of dust concentration, wind speed, and relative humidity on the performance of photovoltaic panels in Tehran," *Energy Sources, Part A: Recovery, Utilization, and Environmental Effects*, vol. 45, pp. 7867–7877, 2019, doi: 10.1080/15567036.2019.1677811.
[50] L. Xu *et al.*, "The influence of dust deposition on the temperature of soiling photovoltaic glass under lighting and windy conditions," *Solar Energy*, vol. 199, pp. 491–496, 2020, doi: 10.1016/j.solener.2020.02.036.
[51] T. Mirzabek, K. Alisher, O. Komronbek, T. Sayorakhon, and F. Nigina, "Evaluating the Effects of Dust Deposition and Ambient Temperature on Photovoltaic Performance in Uzbekistan's Climate," in *E3S Web of Conferences*, 2025, p. doi: 10.1051/e3sconf/202564802018.
[52] Y. Andrea, T. Pogrebnaya, and B. Kichonge, "Effect of Industrial Dust Deposition on Photovoltaic Module Performance: Experimental Measurements in the Tropical Region," *International Journal of Photoenergy*, p., 2019, doi: 10.1155/2019/1892148.
[53] A. Elamim, S. Sarikh, B. Hartiti, A. Benazzouz, S. Elhamaoui, and A. Ghennioui, "Experimental studies of dust accumulation and its effects on the performance of solar PV systems in Mediterranean climate," *Energy Reports*, p., 2023, doi: 10.1016/j.egyr.2023.10.065.
[54] M. Mehdi, N. Ammari, A. A. Merrouni, A. Benazzouz, and M. Dahmani, "Experimental investigation on the effect of wind as a natural cooling agent for photovoltaic power plants in desert locations," *Case Studies in Thermal Engineering*, p., 2023, doi: 10.1016/j.csite.2023.103038.
[55] B. Stankov, A. Terziev, M. Vassilev, and M. Ivanov, "Influence of Wind and Rainfall on the Performance of a Photovoltaic Module in a Dusty Environment," *Energies (Basel).*, p., 2024, doi: 10.3390/en17143394.
[56] A. A. Sher, N. Ahmad, M. Sattar, U. Ghafoor, and U. H. Shah, "Effect of Various Dusts and Humidity on the Performance of Renewable Energy Modules," *Energies (Basel).*, p., 2023, doi: 10.3390/en16134857.

[57] T. Betti, I. Bevanda, I. Marasović, and I. Zulim, “A new approach to comparing photovoltaic simulation software,” *Energy Sources, Part A: Recovery, Utilization, and Environmental Effects*, vol. 45, pp. 6290–6304, 2023, doi: 10.1080/15567036.2023.2215196.
[58] A. Mashaly, M. Elmadawy, M. Elgohary, and A. Shahin, “Novel and cost-efficient design of stand-alone PV system with simulation using PVsyst and experimental validation,” *Sci. Rep.*, vol. 15, p., 2025, doi: 10.1038/s41598-025-28401-y.
[59] S. Shirzad, A. Fazli, W. Zgham, and S. Fatemi, “Design and Development of Grid-Connected Solar PV Power Plant Using PVsyst,” *Academic Journal of Research and Scientific Publishing*, p., 2023, doi: 10.52132/ajrsp.e.2023.52.3.
[60] W. F. Holmgren, C. W. Hansen, and M. A. Mikofski, “pvlib python: a python package for modeling solar energy systems,” *J. Open Source Softw.*, vol. 3, no. 29, p. 884, Sep. 2018, doi: 10.21105/joss.00884.
[61] R. Perez, P. Ineichen, R. Seals, J. Michalsky, and R. Stewart, “Modeling daylight availability and irradiance components from direct and global irradiance,” *Solar Energy*, vol. 44, no. 5, pp. 271–289, 1990, doi: 10.1016/0038-092X(90)90055-H.
[62] D. Faiman, “Assessing the outdoor operating temperature of photovoltaic modules,” *Progress in Photovoltaics: Research and Applications*, vol. 16, no. 4, pp. 307–315, Jun. 2008, doi: 10.1002/pip.813.